Recent intensification of tropical climate variability in the Indian Ocean

NERILIE J. ABRAM[1,2]*, MICHAEL K. GAGAN[1]*, JULIA E. COLE[3], WAHYOE S. HANTORO[4] AND MANFRED MUDELSEE[5]

[1]Research School of Earth Sciences, The Australian National University, Canberra, ACT 0200, Australia
[2]British Antarctic Survey, Natural Environment Research Council, Cambridge CB3 0ET, UK
[3]Department of Geosciences, University of Arizona, Tucson, Arizona 85721, USA
[4]Research and Development Center for Geotechnology, Indonesian Institute of Sciences (LIPI), Bandung 40135, Indonesia
[5]Climate Risk Analysis, Schneiderberg 26, 30167 Hanover, Germany
*e-mail: nabr@bas.ac.uk; Michael.Gagan@anu.edu.au

Published online: 16 November 2008; doi:10.1038/ngeo357

The interplay of the El Niño Southern Oscillation, Asian monsoon and Indian Ocean Dipole (IOD)[1–3] drives climatic extremes in and around the Indian Ocean. Historical[4,5] and proxy[6–9] records reveal changes in the behaviour of the El Niño Southern Oscillation and the Asian monsoon over recent decades[10–12]. However, reliable instrumental records of the IOD cover only the past 50 years[1,3], and there is no consensus on long-term variability of the IOD or its possible response to greenhouse gas forcing[13]. Here we use a suite of coral oxygen-isotope records to reconstruct a basin-wide index of IOD behaviour since AD 1846. Our record reveals an increase in the frequency and strength of IOD events during the twentieth century, which is associated with enhanced seasonal upwelling in the eastern Indian Ocean. Although the El Niño Southern Oscillation has historically influenced the variability of both the IOD and the Asian monsoon[3,8,10], we find that the recent intensification of the IOD coincides with the development of direct, positive IOD–monsoon feedbacks. We suggest that projected greenhouse warming may lead to a redistribution of rainfall across the Indian Ocean and a growing interdependence between the IOD and Asian monsoon precipitation variability.

IOD events occur when the sea surface temperature (SST) gradient and zonal winds along the equatorial Indian Ocean reverse from their climatological state[1,2] (Fig. 1). These changes bring drought to western Indonesia and southern Australia and heavy rains to eastern Africa and southern India, leading to severe impacts on societies and ecosystems[1,2,13–15]. Since the discovery of the zonal IOD pattern[1,2], fundamental questions about its independence from the El Niño Southern Oscillation (ENSO), its natural modes of variability and its interaction with the Asian monsoon have been raised[8,16–19]. The primary cause of these uncertainties around IOD behaviour is the absence of reliable instrumental records from the IOD regions before AD 1958 (refs 1,3) (see Supplementary Information, Fig. S1).

In this study, we use coral records to develop an extended history of SST and rainfall anomalies associated with the IOD (Fig. 1). Coral reconstructions of the IOD have, so far, been limited by the absence of long coral records from the upwelling region along the coast of Sumatra where the strongest IOD anomalies occur[3,8,16]. We use a new monthly record of oxygen isotope ratios (δ^{18}O) extracted from the skeletons of *Porites sp.* corals from the Mentawai Island arc, located ~200 km offshore of Sumatra in western Indonesia. Here, IOD upwelling cools the ambient SST and decreases rainfall[15,20], both of which increase coral δ^{18}O. The new Mentawai coral δ^{18}O record (Supplementary Information, Table S1) spans AD 1858–1997, when the Mentawai reefs experienced widespread mortality[15].

The Mentawai coral δ^{18}O record comes from within the eastern region used to define the Indian Ocean dipole mode index[1] (DMI; Fig. 1). It is complemented by an additional coral δ^{18}O record extending back to AD 1783 from Bali in the south-central Indonesian archipelago[8]. This site lies on the periphery of the

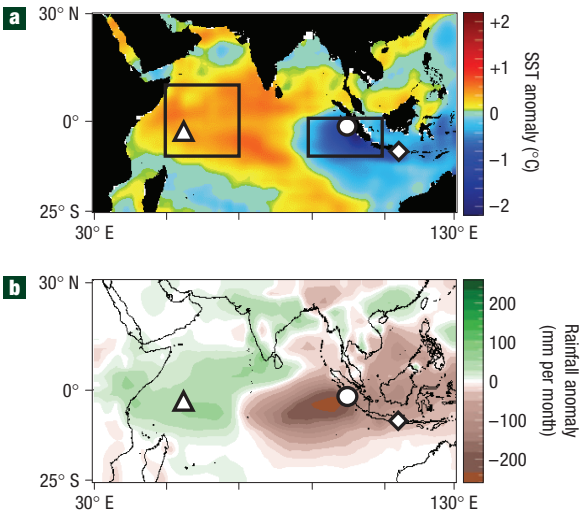

Figure 1 IOD climate anomalies. a,**b**, Composites of SST (**a**) and rainfall (**b**) anomalies for July–November of the 1994, 1997 and 2006 IOD events[21,29]. Boxes mark the eastern and western sectors used to calculate the dipole mode index (DMI) from the zonal difference in equatorial SST anomalies[1]. The locations of coral records from the Mentawai Islands (circles), Bali[8] (diamonds) and the Seychelles[6,9] (triangles) are shown.

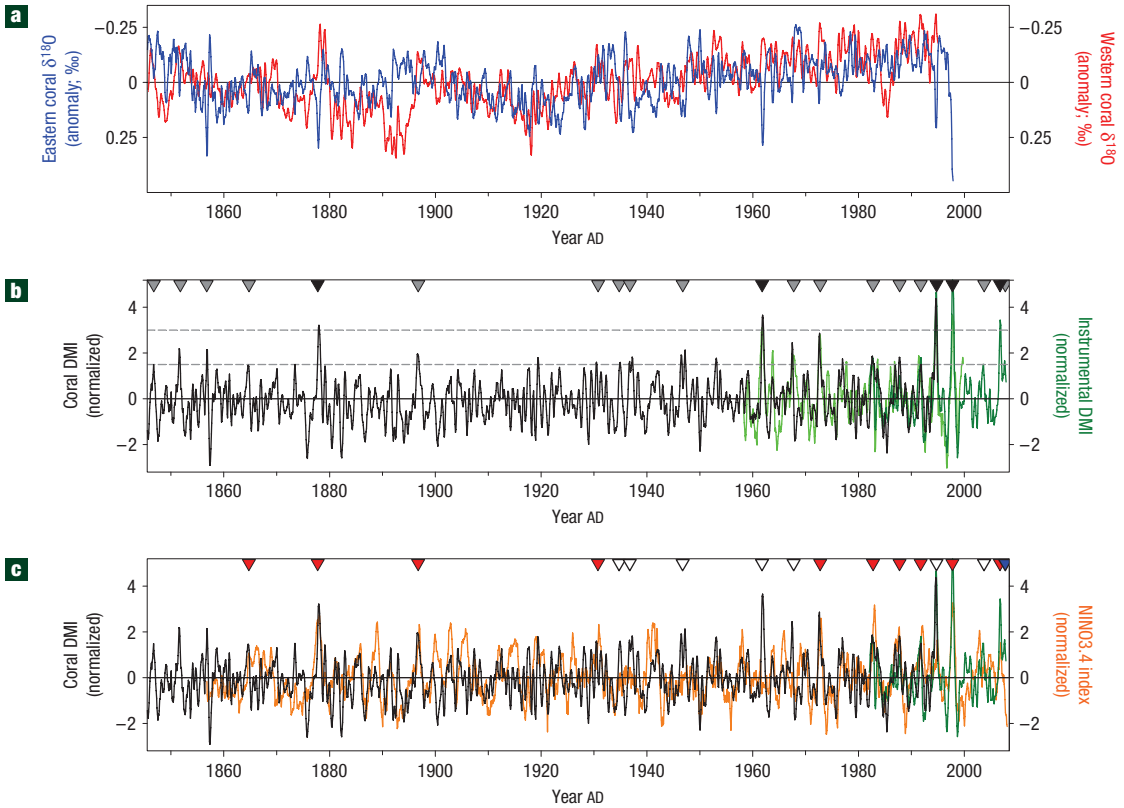

Figure 2 Coral reconstruction of the DMI. a, The $\delta^{18}O$ record for the eastern IOD region (blue) is the average of coral records from the Mentawai Islands (this study) and Bali[8]. The western $\delta^{18}O$ record (red) is the average of two coral records from the Seychelles[6,9]. **b**, The coral DMI (black) is calculated from the east–west difference in $\delta^{18}O$ anomalies (**a**) and has highly significant correlations with instrumental DMI records (light green, Saji DMI; dark green, Reynoldsv2 DMI; Supplementary Information, Fig. S1) (refs 1,21). Triangles mark IOD events that are moderate (grey) and strong (black), where the DMI during July–November exceeds 1.5σ and 3.0σ, respectively. **c**, The extended DMI (black, green) correlates significantly with the NINO3.4 index[5] (orange). Triangles show moderate–strong IOD events that coincide with El Niño events[16] (red, 56%), neutral ENSO states (white, 39%) and La Niña events (blue, 2007 event only). DMIs and NINO3.4 are normalized relative to 1960–1990.

eastern DMI sector[3], but is sensitive to the initial, small-scale upwelling anomalies that can mature and develop along the Sumatran coast into IOD events. In the western DMI sector, two long coral $\delta^{18}O$ records from the Seychelles together extend back to AD 1846 (refs 6,9). Here, IOD events produce warmer and wetter conditions, which both decrease coral $\delta^{18}O$. The combined use of these four coral records enables us to develop a coral DMI (Fig. 2) that reconstructs the east–west difference in ocean temperature and rainfall anomalies across the equatorial Indian Ocean (see Supplementary Information, Tables S2–S4).

The coral DMI correlates significantly with instrumental SST[1,21] and rainfall indices of IOD activity (see Supplementary Information, Fig. S1). Correlation is optimized using July–November averages (correlation coefficients $r_{Saji} = 0.82$, $r_{Reynoldsv2} = 0.92$, $r_{OLR} = -0.87$, $p < 0.0001$) (refs 1,21), which encompass the seasonal timing of IOD events[1–3]. The strong correlations with instrumental indices confirm that the coral DMI closely tracks the coupled ocean–atmosphere signatures of the IOD (see Supplementary Information, Fig. S2). The new coral DMI extends the Saji *et al.* index by 112 years to AD 1846. Since this time the coral DMI (including 1995–2007 data spliced from the SST DMI[21]) identifies 16 moderate ($>1.5\sigma$) and five strong ($>3\sigma$) IOD events.

The coral DMI provides the long-term perspective required to evaluate questions about the dependence/independence of the IOD and ENSO[16]. El Niño events may generate IOD conditions by warming the western IOD region, and also reducing atmospheric convection and decreasing thermocline depth in the eastern IOD sector[8,9,22]. The coral DMI confirms previous studies[3,8] by correlating significantly with indices of ENSO variability. The best correlations are observed with SST anomalies in the NINO3.4 region of ENSO activity[5] ($r_{annual} = 0.44$, $r_{July–Nov.} = 0.51$, $p < 0.0001$; Fig. 2c), and significant coherency exists at biennial, interannual and decadal periods (see Supplementary Information, Fig. S3). On an event-by-event basis, however, only 56% of the moderate–strong IOD events identified in the coral DMI coincide with El Niño events[16]. This supports theories that ENSO teleconnections play an important, but not exclusive, role in driving IOD variability[3,22]. For example, 39% of IOD events occur during years when ENSO was in a neutral state[16] and the 2007 event developed during a La Niña.

The extended IOD history reveals that the frequency of IOD events has not remained constant. A significant increase in the number of moderate–strong IOD events in recent decades is identified using a Gaussian kernel technique[23] to estimate IOD occurrence rate ($p = 0.05$; tested against the null hypothesis of constant occurrence rate) (Fig. 3a). In the mid-nineteenth century the IOD recurrence interval was ~7 years, which declined to a minimum of ~20 years at the start of the twentieth century. The frequency of IOD events then increased through the twentieth century to a recent recurrence interval of ~4 years. The increasing

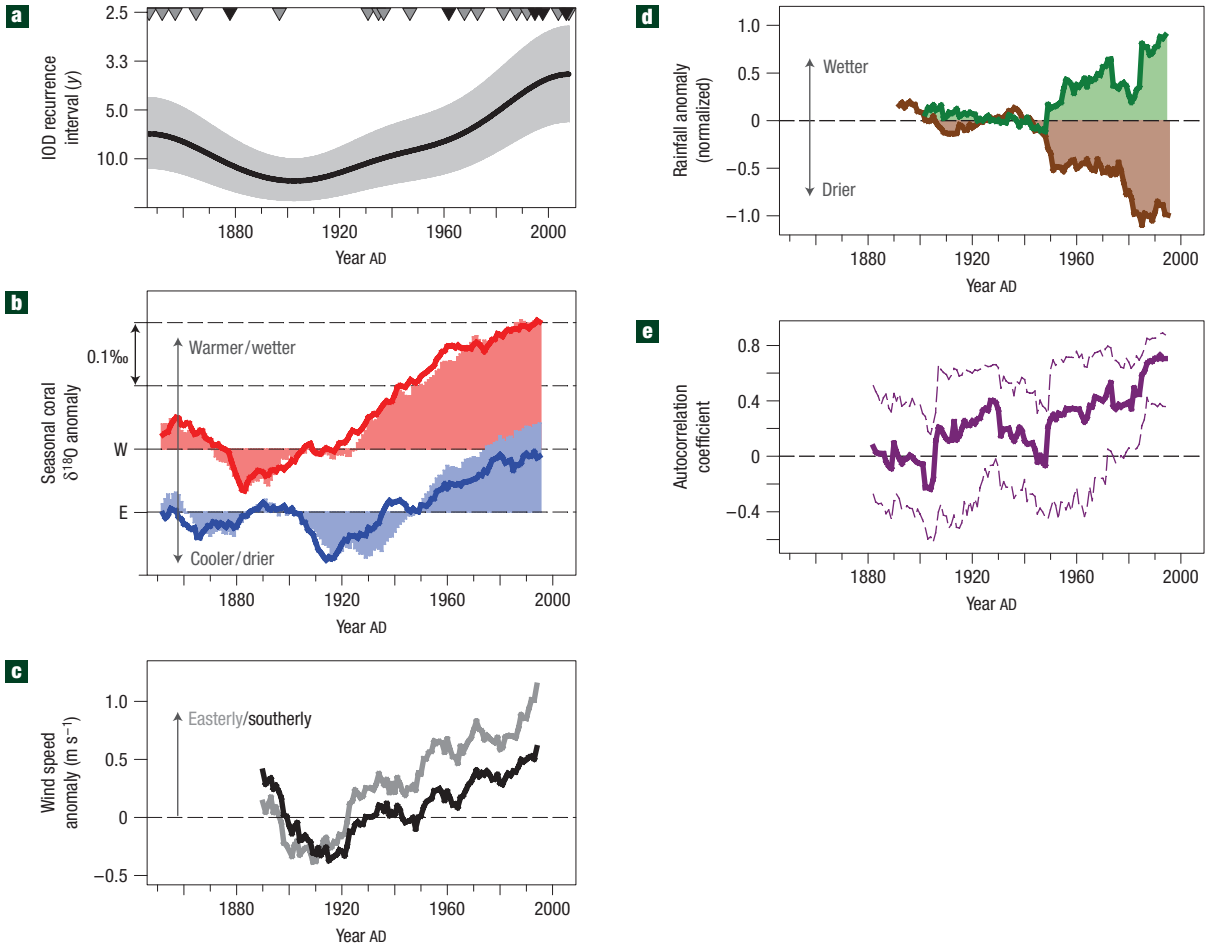

Figure 3 Twentieth-century intensification of the IOD. a, Occurrence rate of IOD events (black curve) using a Gaussian kernel technique[23] with 90% confidence interval (shading) from 2000 bootstrap simulations. The triangles show moderate (grey) and strong (black) IOD events (Fig. 2b). **b**, 25 year moving averages of eastern (blue) and western (red) coral δ^{18}O during the IOD season (July–November; lines) and non-IOD season (March–May; shading), relative to pre-1940 means. **c**, 25 year moving averages of IOD-season zonal (grey, inverted) and meridional (black) wind speed[30] over the eastern IOD upwelling region (90–104° E, 0–10° S), relative to pre-1940 means. **d**, 25 year moving averages of IOD-season rainfall in western Indonesia (brown; five stations in 95–105° E, 0–10° S with >50 years coverage) and eastern Africa (green; 15 stations in 35–45° E, 5° N–5° S with >80 years coverage), normalized relative to the common 1910–1940 interval (Global Historical Climatology Network v2β). **e**, 25 year moving correlation between ENSO-independent residuals of the IOD and Asian monsoon (solid curve), with a 95% Monte Carlo confidence window (dashed curves). The twentieth-century increase in IOD occurrence rate (**a**) has been accompanied by an IOD-season strengthening of the eastern upwelling (**b**) and southeasterly wind speeds off Sumatra (**c**), divergent IOD-season rainfall trends across the tropical Indian Ocean (**d**) and strengthening of direct, positive IOD–monsoon interaction (**e**).

frequency of IOD events is matched by a significant ($p = 0.026$) increase in the occurrence of strong IOD events; four of the five have occurred since 1961, and three of these since 1994. Notably, the occurrence of consecutive IOD events in 2006 and 2007 (ref. 24) is unprecedented in the coral reconstruction.

To examine the physical processes associated with this exceptional twentieth-century intensification of the IOD, we analysed the long-term trends in the coral δ^{18}O records. The seasonal nature of the IOD means that long-term changes can be resolved by comparing coral δ^{18}O anomalies from the IOD season (July–November) with δ^{18}O anomalies from months with no IOD influence (March–May). The Indian Ocean corals show strong warming/freshening trends during the twentieth century (Fig. 3b), consistent with instrumental records of basin-wide warming[25]. In the western region, changes in coral δ^{18}O during the IOD and non-IOD seasons track each other closely and show the same rate of warming/freshening (-0.026‰ decade^{-1} since 1900), suggesting little long-term variation in the strength of IOD processes in the western Indian Ocean. In the eastern Indian Ocean, the rate of twentieth-century warming/freshening during months with no IOD influence (-0.024‰ decade^{-1}) is similar to that in the western sector. However, the key difference is that during the IOD season the δ^{18}O anomalies in the eastern sector show a much weaker trend (-0.016‰ decade^{-1}; the result remains robust if more recent start dates are used). This suppression of twentieth-century warming/freshening during the IOD season suggests that the eastern Indian Ocean has experienced a concurrent increase in the frequency/magnitude of IOD upwelling.

Strengthened upwelling in the eastern IOD sector implies that there has been an intensification of the southeasterly trade winds along the coast of Sumatra, and/or shoaling of the thermocline in the eastern IOD sector[2,16]. Historical ship-based measurements support a twentieth-century intensification of the southeasterly trade winds offshore of Sumatra (Fig. 3c). This is

consistent with theories that preferential greenhouse warming of landmasses will strengthen alongshore winds[26]. This process has been linked to intensified coastal upwelling in other locations[27], and may account for the enhanced upwelling in the eastern IOD region. The influence of twentieth-century warming on long-term changes in the Walker circulation over the tropical Pacific[11] may have also enhanced eastern IOD upwelling. Twentieth-century weakening of the Walker overturning cell has been accompanied by an eastward displacement of convection over Indonesia and shoaling of the thermocline in the Indo-Pacific Warm Pool[11,25]. Both processes are consistent with an intensification of the IOD via the eastern Indian Ocean upwelling region, with reduced convection favouring the development of anomalous surface easterly winds and shoaling of the thermocline assisting upwelling of cooler waters.

The long-term perspective provided by the coral DMI thus demonstrates that there has been an exceptional increase in the frequency and strength of IOD events during the twentieth century associated with enhanced upwelling in the eastern IOD region, which may be attributable to anthropogenic greenhouse warming[11,25–27]. The impacts of this IOD intensification are evident by divergent east–west trends in rainfall across the Indian Ocean basin. Through the twentieth century, IOD season rainfall has progressively decreased in western Indonesia and increased in eastern Africa (Fig. 3d).

The intensification of the IOD raises questions of how its interactions with the ENSO and Asian monsoon systems may have evolved during the twentieth century. Analysis of the temporal evolution of the IOD–ENSO relationship shows that their positive correlation was strong before 1905 and after 1960, but fell below significance between 1905 and 1960 (see Supplementary Information, Fig. S4; Supplementary Information, Table S5). Diminished ENSO teleconnections are evident in both the eastern and western IOD sectors during the 1905–1960 interval[8,9], corresponding to a well documented period of reduced ENSO strength[7]. This suggests that the IOD–ENSO relationship is strongest when ENSO itself is strong[8], although the twentieth-century increase in the frequency of moderate–strong IOD events cannot be explained by ENSO alone (Fig. 2c).

Correlation of the coral DMI with the all-India monsoon rainfall index[4] shows that IOD events were significantly associated with reduced monsoon rainfall before 1905 (see Supplementary Information, Fig. S4). This negative IOD–monsoon relationship is probably an indirect result of the strong inverse relationship between ENSO and the Asian monsoon[10], with El Niño conditions simultaneously promoting reduced monsoon rainfall and IOD events. However, when ENSO teleconnections strengthened again after 1960, the expected negative IOD–monsoon relationship did not return. Instead, analysis of instrumental records indicates that positive IOD–monsoon feedbacks have existed in recent decades. These studies propose that strengthened Asian summer monsoon circulation promotes the development of IOD events by strengthening the zonal Indian Ocean temperature gradient and southeasterly trade winds[19,22], whereas established IOD events strengthen atmospheric convection and monsoon rainfall over southern India[17,18]. The coral DMI suggests that these instrumental records of positive IOD–monsoon feedbacks during recent decades are unusual in the context of longer-term tropical climate behaviour since the mid-nineteenth century.

To assess this further we constructed residual records of the IOD and monsoon by removing the common influence of ENSO (see Supplementary Information, Fig. S4). Moving correlations of the monsoon rainfall residual with the IOD residual show a positive trend through the twentieth century, suggesting a progressive strengthening of direct interaction between the IOD and Asian monsoon (Fig. 3e; Supplementary Information, Table S5). Since ~1960 this ENSO-independent relationship has become significant, such that recent IOD events correspond to monsoons that are stronger than expected on the basis of the influence of ENSO alone. Spatial correlation maps indicate that this direct IOD–monsoon interaction involves IOD-like temperature and wind anomalies in the eastern IOD region (see Supplementary Information, Fig. S5). This raises the possibility that IOD intensification may be associated with the concurrent development of positive IOD–monsoon feedbacks observed in recent decades[17–19].

Multimodel assessments of anthropogenic greenhouse warming indicate that strengthened Asian monsoon rainfall and a more El Niño-like mean state are expected to develop during the twenty-first century[28]. Our results suggest that these changes are likely to be accompanied by increases in the frequency and severity of IOD events, and possibly a strengthening interdependence between IOD and Asian monsoon variability. This new perspective on the dynamic role that the Indian Ocean plays in tropical climate change has profound consequences for the distribution, variability and predictability of future rainfall. Importantly, our findings demonstrate that the equatorial eastern Indian Ocean is particularly sensitive to changes in tropical climate interactions, making this a key region to understand and monitor in studies of past and ongoing climate change.

METHODS

The Mentawai coral cores were slabbed and X-rayed to reveal the annual coral growth bands (see Supplementary Information, Methods; Supplementary Information, Plates S1–S3). Petrographic thin sections show good preservation of the original coral aragonite. Measurements of coral $\delta^{18}O$ were made at the Research School of Earth Sciences, The Australian National University, using a Finnigan MAT-251 mass spectrometer coupled to an automated Kiel carbonate device. Results were corrected using the NBS-19 ($\delta^{18}O = -2.20‰$) and NBS-18 ($\delta^{18}O = -23.0‰$) standards and are reported relative to Vienna Peedee belemnite. Reproducibility of coral $\delta^{18}O$ for ~200 μg samples is ±0.07‰ (2σ, $n = 34$ pairs). The chronologies for the Mentawai coral record and the published records used in this study[6,8,9] were established using annual cycles of $\delta^{18}O$ and verified using annual growth bands. The typical uncertainty on these annual markers is ±1–2 months[6]. The historically documented extreme conditions in the Indian Ocean during 1877 provide a further independent test of the accuracy of the timescales in the early portion of the coral records used in this study.

The coral DMI was constructed following the methods of ref. 1. This involved using a Gaussian filter (frequency = 0.07 ± 0.07 years^{-1}) to remove variability at periods longer than 7 years from each of the coral $\delta^{18}O$ anomaly records. The two coral records from the eastern Indian Ocean[8] were then averaged and subtracted from the average of the two western Indian Ocean coral records[6,9]. The result was smoothed over 5 months and normalized (1960–1990) to produce the coral DMI reconstruction. The method was also applied to the unfiltered coral $\delta^{18}O$ anomaly records to produce an unfiltered coral DMI that retains variability at periods longer than 7 years. The filtered version of the coral DMI was used for comparison with the instrumental DMIs (constructed using the same method), and for identifying IOD events. All other analyses used the unfiltered version of the coral DMI.

Correlation analysis was performed using the KNMI Climate Explorer website (http://climexp.knmi.nl), which uses a Monte Carlo method for determining confidence ranges. Calculation of p-values takes into account autocorrelation of the time series. Correlation results and significance were also verified independently using a block bootstrap method (http://www.mudelsee.com).

Estimates of the IOD and Asian monsoon residuals were constructed using Climate Explorer. For the monsoon residual, the expected influence of ENSO was removed using the linear correlation between June–September (monsoon-season) averages of the all-India rainfall index[4] and NINO3.4 (ref. 5) in the pre-1980 period, when their relationship was strong and relatively stationary[10]. Before 1980, June–September averages of the NINO3.4 index explain 40% of

the variance of monsoon rainfall. Correlations of July–November (IOD-season) averages of the coral DMI and NINO3.4 were used to estimate the IOD residual. Construction of this residual DMI record is supported by the coherent (that is, linear) relationship between IOD and ENSO variability over biennial, interannual and interdecadal periods. NINO3.4 explains 27% of the July–November variance of the coral DMI. Spatial correlation maps for the IOD and Asian monsoon residuals suggest that the ENSO-related signal has been adequately removed (see Supplementary Information, Fig. S5).

Received 18 June 2008; accepted 20 October 2008; published 16 November 2008.

References

1. Saji, N. H., Goswami, B. N., Vinayachandran, P. H. & Yamagata, T. A dipole mode in the tropical Indian Ocean. *Nature* **401**, 360–363 (1999).
2. Webster, P. J., Moore, M. D., Loschnigg, J. P. & Leben, R. R. Coupled ocean–atmosphere dynamics in the Indian Ocean during 1997–98. *Nature* **401**, 356–360 (1999).
3. Saji, N. H. & Yamagata, T. Structure of SST and surface wind variability during Indian Ocean Dipole Mode events: COADS observations. *J. Clim.* 2735–2751 (2003).
4. Parthasarathy, B., Munot, A. A. & Kothawale, D. R. *Contributions from Indian Institute of Tropical Meteorology*, Research Report RR-065, Aug 1995, Pune 411 008, India (1995).
5. Kaplan, A. *et al.* Analysis of global sea surface temperature 1856–1991. *J. Geophys. Res.* **103**, 18567–18589 (1998).
6. Charles, C. D., Hunter, D. E. & Fairbanks, R. G. Interaction between the ENSO and the Asian monsoon in a coral record of tropical climate. *Science* **277**, 925–928 (1997).
7. Urban, F. E., Cole, J. E. & Overpeck, J. T. Influence of mean climate change on climate variability from a 155-year tropical Pacific coral record. *Nature* **407**, 989–993 (2000).
8. Charles, C. D., Cobb, K. M., Moore, M. D. & Fairbanks, R. G. Monsoon–tropical ocean interaction in a network of coral records spanning the 20th century. *Mar. Geol.* **201**, 207–222 (2003).
9. Pfeiffer, M. & Dullo, W.-C. Monsoon-induced cooling of the western equatorial Indian Ocean as recorded in coral oxygen isotope records from the Seychelles covering the period of 1840–1994 AD. *Quat. Sci. Rev.* **25**, 993–1009 (2006).
10. Kumar, K. K., Rajagopalan, B. & Cane, M. A. On the weakening relationship between the Indian Monsoon and ENSO. *Science* **284**, 2156–2159 (1999).
11. Vecchi, G. A. *et al.* Weakening of tropical Pacific atmospheric circulation due to anthropogenic forcing. *Nature* **441**, 73–76 (2006).
12. Goswami, B. N., Venugopal, V., Sengupta, D., Madhusoodanan, M. S. & Xavier, P. K. Increasing trend of extreme rain events over India in a warming environment. *Science* **314**, 1442–1445 (2006).
13. Conway, D., Hanson, C. E., Doherty, R. & Persechino, A. GCM simulations of the Indian Ocean dipole influence on East African rainfall: Present and future. *Geophys. Res. Lett.* **34**, L03705 (2007).
14. Ashok, K., Guan, Z. & Yamagata, T. Influence of the Indian Ocean Dipole on the Australian winter rainfall. *Geophys. Res. Lett.* **30**, 1821 (2003).
15. Abram, N. J., Gagan, M. K., McCulloch, M. T., Chappell, J. & Hantoro, W. S. Coral reef death during the 1997 Indian Ocean Dipole linked to Indonesian wildfires. *Science* **301**, 952–955 (2003).
16. Meyers, G., McIntosh, P., Pigot, L. & Pook, M. The years of El Niño, La Niña and interactions with the tropical Indian Ocean. *J. Clim.* **20**, 2872–2880 (2007).
17. Ashok, K., Guan, Z., Saji, N. H. & Yamagata, T. Individual and combined influences of ENSO and the Indian Ocean Dipole on the Indian summer monsoon. *J. Clim.* **17**, 3141–3155 (2004).
18. Gadgil, S., Vinayachandran, P. H., Francis, P. A. & Gadgil, S. Extremes of the Indian summer monsoon rainfall, ENSO and equatorial Indian Ocean oscillation. *Geophys. Res. Lett.* **31**, L12213 (2004).
19. Swapna, P. & Krishnan, R. Equatorial undercurrents associated with Indian Ocean Dipole events during contrasting summer monsoons. *Geophys. Res. Lett.* **35**, L14S04 (2008).
20. Abram, N. J. *et al.* Seasonal characteristics of the Indian Ocean Dipole during the Holocene epoch. *Nature* **445**, 299–302 (2007).
21. Reynolds, R. W., Rayner, N. A., Smith, T. M., Stokes, D. C. & Wang, W. An improved in situ and satellite SST analysis for climate. *J. Clim.* **15**, 1609–1625 (2002).
22. Fischer, A. S., Terray, P., Guilyardi, E., Gualdi, S. & Delecluse, P. Two independent triggers for the Indian Ocean Dipole/Zonal Mode in a coupled GCM. *J. Clim.* **18**, 3428–3449 (2005).
23. Mudelsee, M., Börngen, M., Tetzlaff, G. & Grünewald, U. No upward trends in the occurrence of extreme floods in central Europe. *Nature* **425**, 166–169 (2003).
24. Luo, J. J., Behera, S. K., Masumoto, Y., Sakuma, H. & Yamagata, T. Successful prediction of the consecutive IOD in 2006 and 2007. *Geophys. Res. Lett.* **35**, L14S02 (2008).
25. Alory, G., Wijffels, S. E. & Meyers, G. Observed temperature trends in the Indian Ocean over 1960–1999 and associated mechanisms. *Geophys. Res. Lett.* **34**, L02606 (2007).
26. Bakun, A. Global climate change and intensification of coastal ocean upwelling. *Science* **247**, 198–201 (1990).
27. McGregor, H. V., Dima, M., Fischer, H. W. & Mulitza, Rapid 20th-century increase in coastal upwelling off northwest Africa. *Science* **315**, 637–639 (2007).
28. Meehl, G. A. *et al.* in *Climate Change 2007: The Physical Science Basis. Contribution of Working Group 1 to the Fourth Assessment Report of the Intergovernmental Panel on Climate Change* (eds Solomon, S. *et al.*) 747–845 (Cambridge Univ. Press, 2007).
29. Xie, P. & Arkin, P. A. Analyses of global monthly precipitation using gauge observations, satellite estimates, and numerical model predictions. *J. Clim.* **9**, 840–858 (1996).
30. Woodruff, S. D., Diaz, H. F., Worley, S. J., Reynolds, R. W. & Lubker, S. J. Early ship observational data and ICOADS. *Clim. Change* **73**, 169–194 (2005).

Supplementary Information accompanies the paper at www.nature.com/naturegeoscience.

Acknowledgements

We thank B. Suwargadi, D. Prayudi, I. Suprianto, K. Glenn, T. Watanabe, H. Scott-Gagan, K. Sieh and the Indonesian Institute of Sciences (LIPI) for logistical support and technical assistance with fieldwork, which was carried out under LIPI Research Permit numbers 3551/I/KS/1999 and 2889/II/KS/2001. We also thank H. Scott-Gagan and J. Cali for laboratory assistance. C. Charles and M. Pfeiffer are thanked for providing published coral data. This study was supported by an Australian Postgraduate Award and RSES Jaeger Scholarship to N.J.A., and an Australian Research Council grant (DP0663227) to M.K.G. and W.S.H.

Author contributions

N.J.A. was responsible for coral geochemical analysis and interpretation of the records. M.K.G. was Chief Investigator and the Australian Institutional Counterpart for the ARC project. J.E.C. provided the spectral analysis. W.S.H. was Partner Investigator and the Indonesian Institutional Counterpart for the ARC project. M.M. assisted in statistical analysis. N.J.A., M.K.G. and J.E.C. wrote the paper.

Author information

Reprints and permissions information is available online at http://npg.nature.com/reprintsandpermissions. Correspondence and requests for materials should be addressed to N.J.A. or M.K.G.